Research Article

Ibrahim A. Alnaser and Mohammed Yunus*

Enhancement of hardness and wear strength of pure Cu and Cu-TiO₂ composites via a friction stir process while maintaining electrical resistivity

https://doi.org/10.1515/rams-2023-0168 received September 28, 2023; accepted December 27, 2023

Abstract: The study aims to enhance the hardness and wear of copper and Cu-TiO₂-based composites while maintaining high electrical conductivity through friction stir processing (FSP). It assesses the impact of TiO2 volume fractions and groove widths (GWs) on the wear, hardness, resistivity, and microstructure of FSPed Cu and FSPed Cu-TiO₂ surface composite. The samples obtained from the stir zone showed an increase in microhardness of the Cu-TiO₂ surface composite due to particle refinement, uniform distribution, and efficient sticking of TiO2 with Cu. Furthermore, the wear rate increased with decreasing TiO₂ volume fractions in the composite. The worn surface microstructural analysis indicated a transition from harsh to gentle wear with increasing TiO2 volume fractions and GWs. The average grain size reduced significantly in reinforced stir zones compared to pure Cu, and particle size decreased further with increasing groove size. Hardness increased by 25 and 50% compared to unprocessed Cu, but only a negligible increase in electrical resistivity (2.3% Ω m) after FSP.

Keywords: electrical resistivity, surface composites, wear resistance, Cu-based surface composites, friction stir processing

1 Introduction

This unique structure allows for high thermal conductivity,

Copper (Cu) is an exceptionally electrically conductive material with a face-centered cubic (FCC) crystal structure.

Mechanical Engineering, Umm Al-Qura University, Makkah 24372, Saudi Arabia, e-mail: myhasan@uqu.edu.sa Ibrahim A. Alnaser: Department of Mechanical Engineering, College of Engineering, King Saud University, Riyadh 11421, Saudi Arabia, e-mail: ianaser@ksu.edu.sa

* Corresponding author: Mohammed Yunus, Department of

resistance to corrosion and oxidation, ease of joining, and good ductility. Additionally, Cu is a long-lasting and fully recyclable metal [1]. However, its mechanical and wear resistance properties are reasonably low, necessitating improvement. One way to enhance the characteristics of Cu is through the use of Cu metal matrix composites (CMMCs), which can be fortified with various elements such as SiC, TiC, WC, TaC, TiB₂, AlN, Al₂O₃, MWCNT, and CNT [2]. Different methods can be employed to improve the qualities of copper, including alloying and composite preparations.

Nevertheless, it is essential to note that elements like Ni/ Zn can reduce electrical conductivity [3]. Another method used to improve the properties of copper-based alloys is precipitation hardening, which involves incorporating beryllium, nickel, chromium, and zirconium. Fine, coherent, and evenly dispersed precipitates are formed through aging treatment in Cu-Cr-Zr alloys, improving wear resistance and hardness [4]. However, these alloys may exhibit adhesive and abrasive wear characteristics under conditions without lubrication. Extensive research has been conducted on the equal channel angular pressing (ECAP) method, demonstrating the ability to reduce grain size in Cu-Cr-Zr alloys, enhance tensile characteristics, and improve strength. However, as strength increases, ductility decreases [5]. Additionally, the processing of Cu-Cr alloys using ECAP and cold rolling has led to the formation of refined grains and increased strength, but at the cost of decreased electrical conductivity [6]. Li et al. studied a Cu-0.1 wt% Zr alloy that was treated using the ECAP technique. The results revealed high Vickers microhardness values and reduced grain size [7]. Furthermore, friction stir processing (FSP) is a solid-state process utilized to enhance the mechanical characteristics of substances, specifically the CMMC. It has been extensively studied for its ability to increase Cu's mechanical properties and electrical conductivity. Research indicates that increasing the traverse speed can further improve the mechanical properties and reduce grain size, making it suitable for applications that require high strength and high electrical conductivity, such as sliding surfaces, electrical terminals, and switches [8].

FSP can also be used to increase the surface area of Cu, resulting in higher ultimate strength, elongation, and reduction in particle size. Researchers have also explored the use of ceramic particles to reinforce CMMCs. However, creating high-density composite materials using traditional liquid metallurgical methods remains problematic due to differences in melting temperatures and element densities [9]. FSP involves cutting a groove or hole in a metallic plate and filling it with specific metallic or ceramic reinforcing particles. A spinning tool with the appropriate size and axial force is then used to deform the material, forming metal matrix composites (MMCs). The fabrication of Cu/SiC composites has shown that increasing the number of passes improves wear characteristics and mechanical strength due to the homogeneous dispersion of SiC particles. However, the presence of SiC particles reduces the electrical conductivity of the composites [10]. Investigating the FSP of Cu/B₄C composites, it was found that increasing the B₄C particle volume % enhances the microhardness and wear resistance of the composite [11]. An empirical relationship was developed to predict the mechanical behavior of Cu composites as well as the wear resistance qualities supplemented with various particles, including B₄C, Al₂O₃, SiC, WC, and TiC [12]. Y₂O₃ particles increased the mechanical characteristics of Cu/Y₂O₃ composites, whereas Cu/WC composite improved their microstructure, mechanical, and thermophysical properties due to WC particles and the number of passes. FSP used to create a Cu/TiC composite with fine-grained microstructures, and homogeneous dispersion of TiC reinforcement particles, improving the wear resistance of the composite [13,14]. It was demonstrated that adding Al₂O₃ particles and increasing the volume percentage enhanced the microhardness and tensile strength of the Cu/Al₂O₃ composite [15]. The effect of carbon nanotubes (CNTs) on Cu using FSP was studied, and it was found that increasing the number of passes resulted in improved hardness and reduced wear rate [16]. In order to optimize the mechanical and wear characteristics of the treated zone in FSP, it is necessary to investigate several process variables. The Taguchi design of the experiment technique, which utilizes an orthogonal array, can be beneficial in analyzing the influence of process components, minimizing trial trials, and obtaining optimized process parameters. Taguchi's method inspected the impact of various process factors on the mechanical characteristics of various composites, such as Al alloys and Cu composites reinforced with SiC, Gr, and Al₂O₃ particles. These studies found that various process factors significantly impacted the mechanical characteristics of the tested composites [15,17–19]. This work compares the mechanical behavior and microstructural properties of SiC-Gr- and WC-Gr-reinforced Cu matrix hybrid composites. Hard ceramic materials have better

tensile behavior and microhardness, with WC-Gr composites exhibiting the best characteristics [20].

Based on the existing published literature, only a few investigations have been conducted on copper-TiO₂ composites [21]. The FSP process was also used to create comparable surface composites with varying proportions of micron-sized Al₂O₃ ceramic particles. They determined that the tensile properties of the composites improved as the amount of reinforcing phase increased. However, more extensive studies on producing copper-ceramic-based composites using FSP are needed, particularly for a detailed understanding of the microstructure and texture evolution [22]. The study investigates the dynamic compressive behavior of aluminum alloy Al–Si₇Cu₃Mn_{0.5} (LM27) composites manufactured using stir casting with different weight percentages and sizes of SiC and TiO2. The composites were evaluated using a split Hopkinson pressure bar at strain rates of 700, 1,500, and 2,500 s⁻¹. The study found that the fine particle-reinforced composites had higher micro-hardness and maximum strength at higher reinforcement particle concentrations. The dynamic compressive behavior was found to be dependent on the elastic modulus degradation, stress localization, and debonding characteristics [23]. This study aimed to produce a copper-zirconia oxide composite through FSP and examine its effects on the microstructure, mechanical properties, and wear behavior. The results showed a uniform distribution of zirconia particles, a fine grain structure, no alterations in the particle size or shape during processing, strong bonding between copper and zirconia oxide, higher hardness compared to base copper, lower hardness near processed sections, higher friction coefficient, and less wear loss compared to copper [24]. Additive manufacturing (AM) is a novel process involving layer-by-layer manufacturing of 3D CAD-based objects, such as MMCs. This article summarizes current investigations on powder-based AM-generated MMCs, emphasizing their benefits and drawbacks. AM can solve reinforcement/matrix bonding issues, build functionally graded composite materials, and produce geometrically complex products. Rapid cooling, matrix, and reinforcement expansion efficiency, processability, and a lack of suitable parameters for defect-free AM MMC manufacture are all issues [25].

Previous studies have demonstrated that adding ceramic reinforcements to copper surfaces using FSP can improve their mechanical and wear characteristics. Incorporating reinforcements based on oxides has been used relatively infrequently in most studies, which have used other types of reinforcements. Furthermore, other crucial aspects like groove width (GW) and the volume percentage of reinforcements are frequently ignored in these studies. This study intends to develop high-performance Cu. Friction-stirred Cu

and friction-stirred Cu-TiO₂ surface composites under various welding conditions, including GWs and nanoparticle volume percentages, are studied. In order to better understand how these circumstances and the addition of TiO2 nanoparticles affected the final stirred regions in Cu sheets, we will focus on their hardness, wear resistance, electrical characteristics, and microstructures.

2 Methods and materials

This study focuses on improving the wear, mechanical, and surface characteristics of pure Cu and Cu-titanium oxide (TiO₂) composites using FSP. This section presents the experimental work, materials, and equipment used to assess the developed material's performance. The base material (pure Cu) was chosen, and the composition of its constituents was established using scanned electron images (Table 1). Materials were supplied from Nano Research Lab, India. TiO2 nanoparticles with an approximate size of 50 nm were chosen as the reinforcing substance (refer to Figure 1). The microstructural features of Cu and TiO2 particles were observed through scanning electron microscopy (SEM) examination.

This research investigated the impact of adding TiO₂ nanoparticles at the weld location. To achieve this, a lengthwise groove measuring 0.5, 1, and 1.5 mm in width and 3 mm in depth was created at the interface of the two workpieces, and TiO₂ particles were filled into this groove. The properties of the TiO₂ nanoparticles are listed in Table 2. Test samples were prepared from $5 \times 50 \times 120 \,\mathrm{mm}$ dimensioned Cu plates. An EDM (Mitsubishi FA) was used to create a 3 mm deep groove in the middle of the plate, which was then filled with TiO₂ powder. A pinless WC tool was used to cover the groove's top to prevent particle overflow while stirring during the first stage of two-stage FSP [21]. The surface composite was formed in the succeeding step using an FSP tool (Table 3) constructed of WC material with the parameters shown in Figure 2a and b. The stirring machine was utilized for the experiments with several process variables (Table 4): rotational speed of 600 rpm and traverse speed of 50 mm·min⁻¹ [26].

Three plates were submitted to FSP with variable GWs to include different volume percentages of TiO₂ particles (6, 18, and 24% by volume) (Figure 1). The actual and predicted volume

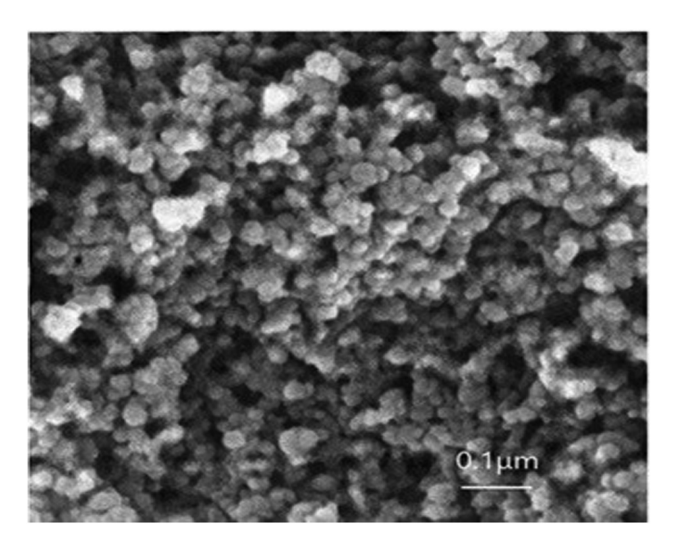


Figure 1: SEM image of TiO₂ nanoparticles.

fractions of TiO₂ components were estimated using the relationship presented in Eqs. (1) and (2) [27]. FSP was carried out on the prepared plates based on the procedure parameters:

Theoretical volume fraction(
$$V_{th}$$
)
= (GW × depth of groove/diameter × length of tool pin) × 100,

Actual volume fraction(
$$V_{ac}$$
) = (GW × depth of groove /area of surface composite) × 100.

Cu plates were welded together, and Cu plate grooves were reinforced with nanomaterials under various conditions to investigate the impact of welding conditions (parameters), such as GW and volume % of nanoparticles, on the microstructural and mechanical properties of the resulting welds. Table 5 lists the various FSP examples studied as determined by GW and TiO2 volume %.

2.1 Characterization of the FSP region

2.1.1 Vickers microhardness measurement

The ground and polished surface of the processed region samples of size 12 mm × 12 mm × 5 mm were prepared

Table 1: Composition of constituents of Cu [21]

Cu	Со	Cr	Si	Ni	Fe	Mn	Р	Sn	Pb	Zn
Base metal	1 × 10 ⁻²	<2 × 10 ⁻³	<5 × 10 ⁻³	<1.1 × 10 ⁻³	1 × 10 ⁻²	1 × 10 ⁻²	22 × 10 ⁻³	<4.1 × 10 ⁻³	<5 × 10 ⁻³	<9 × 10 ⁻³

Table 2: Properties of TiO₂ nanoparticles [22]

Density (g·cm ⁻³)		Melting point (°C)	Specific surface area (m²·g ⁻¹)	Pure volume (cc·g ^{−1})	Mean crystallite size (nm)	Mass percent (%)	
Bulk 0.04–0.06	True 3.9	1,830–1,850	189	0.17	7.52	Ti 44.67	O 55.33

Table 3: Chemical composition of H13 tool steel

Element	С	Mn	P	S	Si	Cr	V	Мо	Fe
wt (%)	0.32-0.45	0.2-0.5	0.03-max	0.03-max	0.8-1.2	0.47-5.5	0.8-1.2	1.1–1.75	Balance

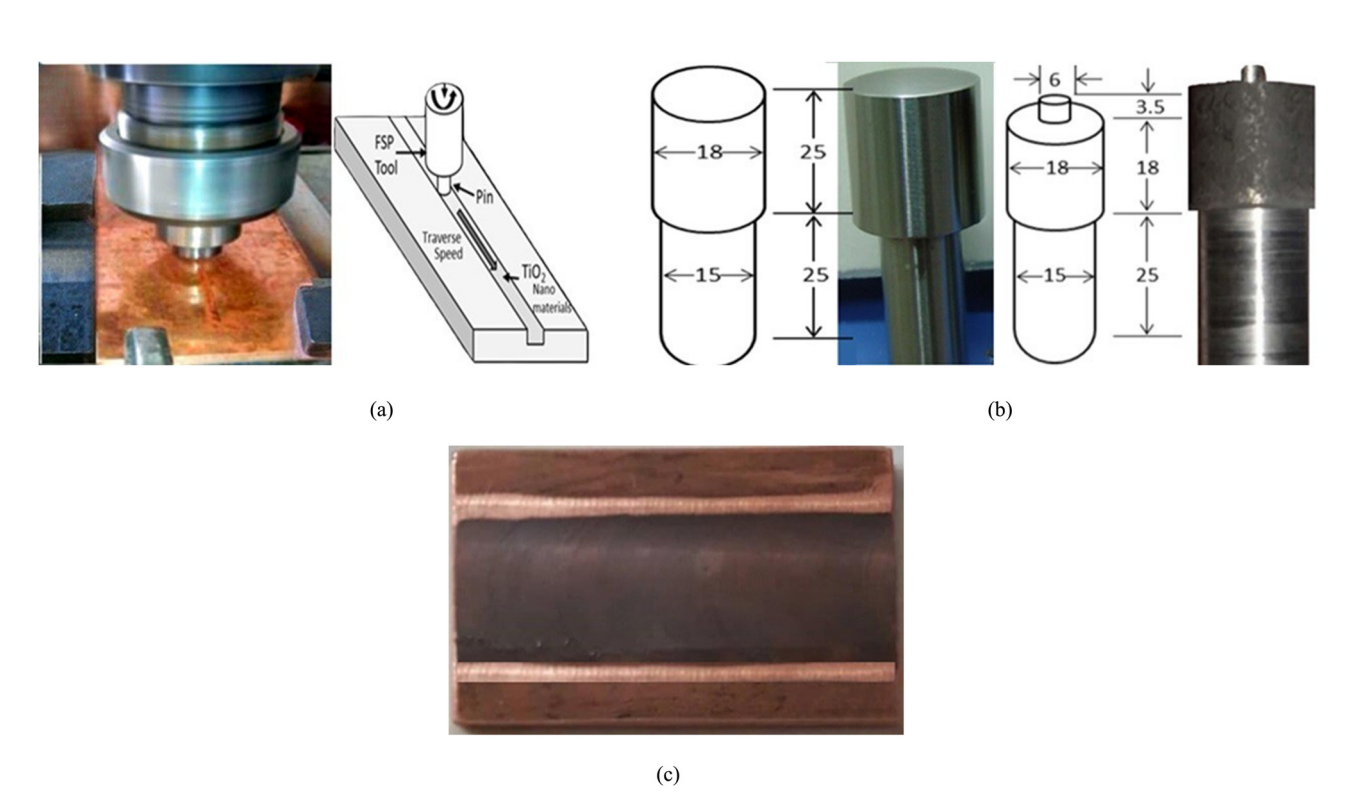


Figure 2: (a) FSP setup with FSP tool and (b) dimensional representation of pinless and pin FSP tool, and (c) prepared FSPed wear sample.

Table 4: FSP parameters were kept constant during experiments

No.	Parameters	Chosen value		
1	Tool pin profile	Straight cylindrical		
2	Pin length	3.5 mm		
3	Tool pin diameter	6 mm		
4	Tool shoulder diameter	18 mm		
5	Tool tilt angle	2.5°		
6	Tool vertical force	6 kN		

Table 5: Various FSP examples considered

Investigated cases	GW (mm)	Volume% of TiO ₂
Α	Pure Cu with 0	0
В	FSPed Cu with 0	0
C	0.5	8
D	1.0	16
E	1.5	24

(following ASTM-384). Vickers microhardness measurements were taken at the mid-plane of the processed cross-section of every 0.5 mm at a load of 200 g with a dwell time of 15 s.

2.1.2 Wear test

The processed samples were tested using a pin and a disk wear testing device (DUCOM TR20, India) to determine how they would wear out in sliding. According to the ASTMG99-04a standard, this testing was carried out at room temperature. The samples, with dimensions of 3 mm × 8 mm × 20 mm, were taken from the processed zone and then prepared by grinding and polishing to produce a smooth surface. The pin-type sample was slid against a hardened steel (EN31) disk with a Rockwell hardness of 63RC during the wear test, which involved sliding the samples at a speed of 1.5 m·s⁻¹, a steady force of 30 N, and 1,000 m sliding distance (SD). The wear rate was calculated by dividing the volumetric loss by the SD and force applied. SEM analysis was done on the wear-out surface of specimens to obtain the morphology.

2.1.3 Electrical resistivity test

Electrical conductivity (reciprocal of resistivity) measurements were performed on samples from the stirred zone. A SIGMASTONE 4-point probe measurement device with 1.6 mm spaced apart probes arranged linearly was employed to assess the sample's electrical resistivity. The resistivity, inversely proportional to conductivity, is expressed as Ωm . A constant current is sent through the two probes to calculate the potential drop V across the middle two probes [28] employing Eq. (3).

$$\rho = R\pi r^2/L,\tag{3}$$

where L, r, and R are the length (m), radius (m), and resistance (ohm) of wire made of Cu, FSPed Cu, and FSPed Cu-TiO₂, respectively

3 Results and discussion

This section presents the results of the microstructure, microhardness, electrical resistivity (reciprocal of conductivity), and wear rate of Cu-TiO₂ composites fabricated through FSP. The effects of GW and volume percentage on these properties are examined.

3.1 Microstructural studies

The research focuses on the fabrication of surface-level nanocomposites using FSP. SEM (Make: Zeiss, Jena, Germany) was used to assess the weld zones and particle sizes. Because the advancing side moves quicker than the retreating side, the stir zone extends somewhat toward the advancing side (right side). In the case of a GW of 1mm, the stir zone expands toward the right, and the entire zone also moved slightly to the right. It could be explained by how quickly one side moves forward compared to how slowly the other retreats.

During FSP, the grain size of the base metal decreases due to dynamic recovery, geometric, and discontinuous recrystallization. During recrystallization, the homogeneous dispersion of TiO₂ in the plasticized matrix nucleates Cu grains. The stirring motion fractures and distributes the components in the matrix uniformly, resulting in a refined grain microstructure. The microstructure study confirms that the TiO₂ particles in the composite did not agglomerate or cluster (refer to Figure 3b).

SEM analysis of the microstructural properties of FSPtreated Cu and Cu/TiO₂ composites showed that the composites with a zero-GW (no reinforcing) have no defects, suggesting a high-quality surface area (Figure 3a). Composites with 1 mm GW (16% TiO₂) exhibit finer dispersion of titanium dioxide particles in Cu. In some areas, composites treated with a high-volume percentage of TiO₂ particles (24%) exhibit minor agglomeration.

The FSPed surface composite exhibits substantial interface bonding between Cu and TiO2, which is predicted to improve the composite's mechanical characteristics. A higher GW results in a high-volume percentage of TiO₂ particles, which increases the flow stress in the plasticized Cu alloy, resulting in insufficient flow. At a GW of 1 mm, the fine dispersion of hard state particles to the Cu metal occurred.

Pure, unprocessed copper has a coarse grain structure, whereas composite materials containing 8, 16, and 24% TiO₂ have a finer grain structure. Dynamic recrystallization occurs as a result of the rotating FSP tool's frictional heat input and plastically deformed material surrounding the stirring pin. The copper matrix may experience a reduction in grain size because of the addition of TiO2 particles. SEM micrographs (Figure 3c and d) show that the interparticle distance between the reinforced TiO₂ particles decreases as the reinforcement volume increases. The even distribution of reinforcements depends on process characteristics like tool rotating and traverse speeds. The interface bond between the matrix and reinforcement material significantly impacts the mechanical characteristics of the composite [29,30].

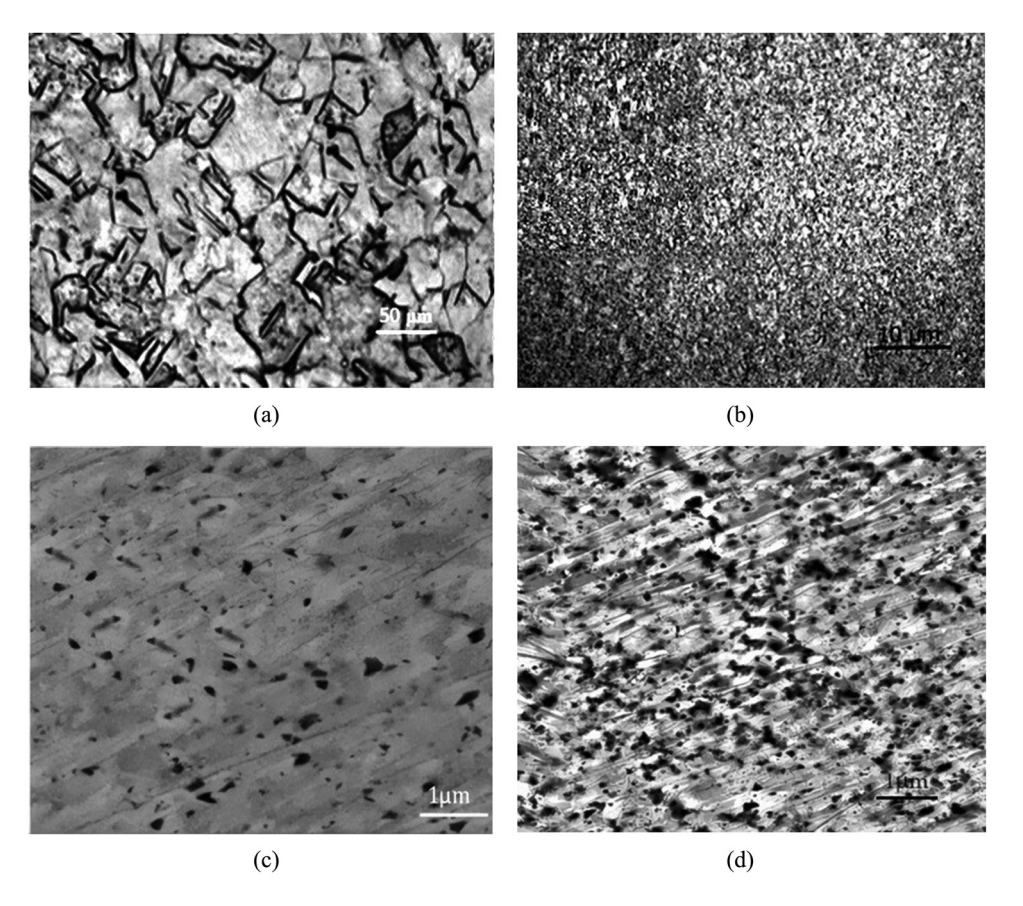


Figure 3: SEM images of (a) FSPed Cu and (b) FSPed Cu–TiO₂ with GW of 0.5 mm and 8 vol% at lower magnification, and FSPed Cu–TiO₂ with (c) GW of 1 mm and 16 vol% and (d) GW of 1.5 mm and 24 vol%.

3.2 Hardness test

Figure 4 illustrates the Vickers microhardness profiles obtained for various FSPed samples.

An instrument made by Vickers was used to assess the samples' microhardness. A 62H_V average hardness was found for the pure Cu metal. According to Section 3.1, grain refining and subsequent heat generation had the most impact on the hardness of FSPed Cu sheets. Because of the TiO₂ particles' homogeneous distribution along the matrix's grain boundaries, the surface composites made via FSP showed fine grain refinement. In the course of solidification, this constrained the grain expansion. In Figure 4, the hardness of the received Cu is displayed together with the average H_v values in the section of the nanocomposites' stirred region. Due to the dispersion of small TiO₂ particles with a size of 50 nm, the nanocomposites always displayed greater hardness values than FSPed Cu. Particle size and heat production are crucial factors to amplify the surface hardness of FSPed composites. The hardest sample in this investigation was produced with a 1.5 mm GW and a 24 vol%, yielding 124 H_V and 121 H_V ,

respectively, with 50 nm TiO_2 particles. These values were around 50 and 45% higher than those of the pure Cu matrix, respectively. According to Figures 4 and 5, the increased hardness was attributable to the finer diffusion of the TiO_2 particles; no intermetallic compounds were identified

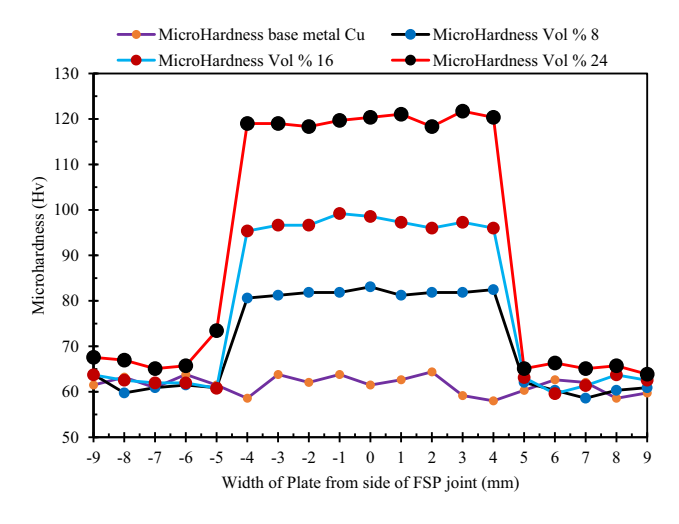


Figure 4: Variation of microhardness along the width of a plate.

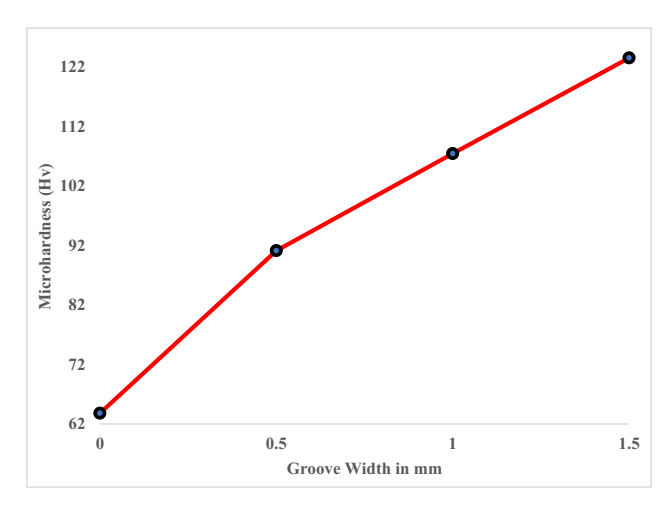


Figure 5: Average microhardness varying with a GW.

during FSP, and the tiny-sized particles were present in the stirred region of the Cu matrix (refer to Figure 3c and d) [30].

The increasing hardness in the surface region can be ascribed to the dispersion of hard state TiO_2 particles, grain refinement in the stir zone, hardening owing to the disparity in temperature reduction between TiO_2 and Cu and

hardening brought on by strain misfit reason for the increase in hardness in the surface region between the pure plastic Cu and elastic ${\rm TiO_2}$. It is commonly noticed that the Hv of the workpiece falls with an increase of heat input during the welding process due to the influence of heat transfer on grain size, as larger grains are associated with reduced material hardness.

In the surface of the FSPed nanocomposite, the stir region achieves the highest hardness level due to two recrystallization events and extreme fine-graining. The study revealed a significant variation in hardness across different welding conditions. However, in general, the hardness in the stir region increased due to grain size reduction, and because of the quenching hardening impact, an increase in TiO₂ % volume in the Cu material may enhance the hardness of the composite [31].

3.3 Wear behavior of FSPed Cu and FSPee Cu/TiO₂ surface composites

SEM images of the worn-out surfaces (Figure 6b) show several deeper and uninterrupted grooves due to FSPed

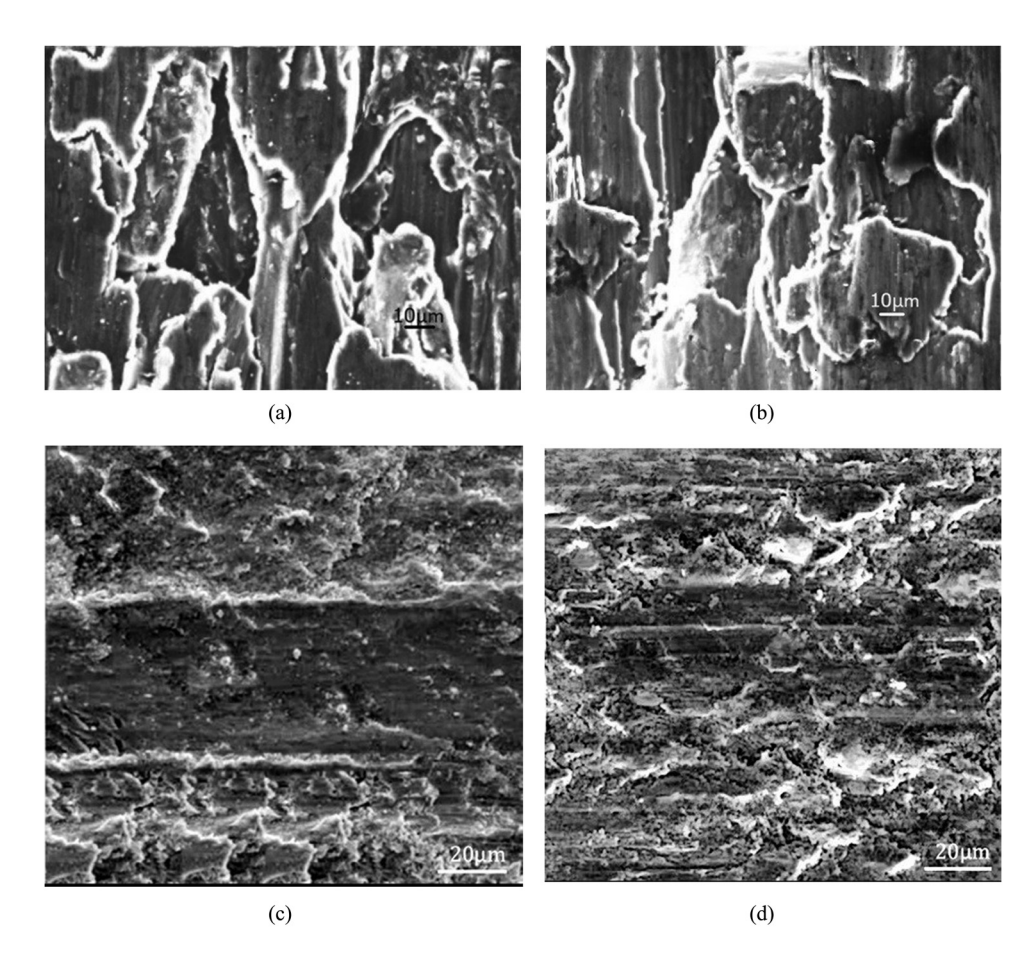


Figure 6: Morphology of worn-out surfaces of (a) pure Cu, (b) friction stirred Cu, (c) Cu–TiO₂ with a grove width of 0.5 mm and 8% vol, and (d) Cu–TiO₂ with a grove width of 1.5 mm and 24% vol.

Cu having a relatively soft surface. The wear-out surface of composites with GWs (0.75 and 1.5 mm) (Figure 6b and c) display increased material removal compared to the FSPed Cu surface, indicating a higher degree of plastic deformation. This discrepancy in material removal is primarily due to differences in surface microhardness [1,29,30]. The Cu FSPed surface with zero GW directly interacts with the mating face since there are no solid particles that might slow the wear. In contrast, the surface is less likely to bend plastically when stiffeners are implanted in copper (as in Figure 6b with a 0.75 mm-wide GW), reducing the material removed during the cutting process. As illustrated in Figure 6d with a GW of 1.5 mm, the degree of deformation also dramatically lowers as the number of TiO2 particles increases, as demonstrated by the observed surface plowing on worn surfaces. Wear tests were performed to evaluate the wear qualities using a pin-on-disk tribometer with a load of 30 N and a sliding speed of 1.5 m·s⁻¹. Wear rates were computed for specimens with various GWs (Figure 7). The wear rate was determined to be $373 \times 10^{-5} \,\mathrm{mm}^3 \cdot \mathrm{m}^{-1}$ for FSPed Cu: however, it decreased to 175.31 × 10⁻⁵ mm³·m⁻¹ for the Cu-TiO₂ composite with a volume of 24% [21]. It is important to note that wear resistance increases as GW decreases, proving that using TiO₂ as reinforcement significantly lessens the wear. This enhancement can be attributed to the composite's improved hardness, brought on by the TiO2's homogeneous dispersion and finely tuned grain structure. Because a hard surface resists plastic deformation better than a softer one, materials with increased hardness exhibit higher wear resistance. Additionally, good interfacial bonding and uniform reinforcement distribution contribute to enhancing wear resistance [1].

The wear rate of pure Cu was greater than that of FSPed Cu without reinforcement. The increased hardness value decreased the wear rate when ${\rm TiO_2}$ ceramic particles were added to a Cu matrix. Due to the uniform distribution

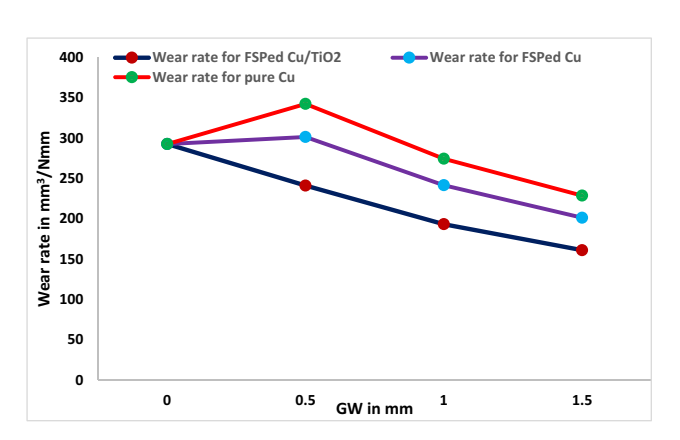


Figure 7: Wear rate variation for different GWs.

of reinforcement and dynamic recrystallization of the base material, the composite's hardness was increased. In proportion to the TiO2 content, the composite's wear resistance increased. Including reinforcement particles reduced the effective contact area between the composite pin and counter disc. Adhesive and abrasive wear were the main wear processes during sliding, according to the composite pin's worn-out surface, as seen under an SEM. Cu's soft and ductile nature contributed to adhesive wear, and sliding Cu against hard rotating steel discs caused plastic deformation, hastening material loss from the sliding surface. On the worn surface, there were deep grooves and delaminations. The heat produced between the Cu and disc softened the Cu, making it easier for debris and hard asperities to penetrate. Increased wear resistance of the material is indicated by the grooves' depth gradually decreasing. The composite's hardness was improved by adding more reinforcement, making it more difficult to penetrate from the surface. TiO2 was visible from the composite image of the worn-out surface as the wear debris formed during sliding fused onto the surface [27,30].

The pin specimen weight loss and wear rate were measured and compared with the substrate. With consistent microhardness, a 1 mm GW exhibited the most minor weight loss, 35% less than the substrate. Abrasive wear is the most common wear mechanism in Cu, and several factors contribute to its higher wear resistance, including the addition of TiO₂ nanopowder, grain size reduction through FSP, and increased microhardness. A specimen with high GW and volume has demonstrated minor weight loss, with a weight loss improvement of around 60% compared to the substrate. The higher pin hardness and similarity to the disc hardness contributed to the reduction of abrasive wear. The friction coefficient per distance varied for different specimens, including the substrate and GWs of 0, 0.5, 1, and 1.5 mm. Pure Cu had a friction coefficient of 0.30, while the other specimens had a friction value of around 0.33. The friction coefficient in 0 and 1 mm increased from 0.3 to 0.33 mm after an SD of 1,000 m, indicating wear and loss of FSP area. The increased variations in friction coefficient can be attributed to higher adhesion in non-FSPed pure copper specimens compared to different GWs [26].

The wear properties of Cu in its as-received state, Cu, after being subjected to FSP and nanocomposite layers were investigated. The Cu matrix of the devised composites contained a fine dispersion of nanoscale TiO₂. In contrast to pure Cu and FSPed Cu, these composites prevented direct loading interaction between the Cu–TiO₂ surface nanocomposite and the disc because they contained a load-bearing component. A 1,000 m slide and various sample coefficients of friction were also examined. The

repeating band formation in the tool travel direction and the gathering and removing wear debris on the worn-out track caused significant variations in the friction coefficients. The average friction coefficients for stirred nanocomposites, stirred processed, and pure Cu were 0.343, 0.332, and 0.30, respectively.

TiO₂ was evenly distributed in the stirred region of the FSP, and a cluster of blind holes served as a grain depositing mechanism. The presence of nano-sized TiO₂ particles in the composite samples was found. Figure 7c and d depicts the debris left behind after the Cu matrix was oxidized and removed and the separation of TiO₂ particles from the stirred region during the wear test. This led to abrasive wear as the main wear mode in the surface composite layers. Frictional heat raised the temperature of the worn surface, which led to dislocation and plastic deformation inside the surface layer of the composite materials. Because of the temperature increase, the oxide layer and worn-out dirt mixed with the soft Cu matrix grow a "mechanical mixed layer" (MML) on the weary face. Oxidation was essential for stabilizing the MML and significantly lowering the finish surface composites' wear rates [30].

Conversely, the existence of coarse TiO_2 nanoparticles and their poor integrity with the Cu matrix caused the MML in the nanocomposite to delaminate. Figure 5d depicts a reduced amount of debris, suggesting that the Cu– TiO_2 nanocomposite layers are more resistant to wear. The superior wearing resistance of the Cu– TiO_2 nanocomposite is due to several factors, including a higher proportion of nano-sized TiO_2 particles, strong bonding between the nanoparticles of TiO_2 and the Cu matrix, a higher microhardness value as a result of the nanosized TiO_2 particles, TiO_2 's ability to withstand wear loads, and prevented direct load contact between Cu and the disc.

3.4 Electrical resistivity

Figure 8 shows the electrical resistivity (Ω m) of Cu, FSPed Cu, and the surface composite FSPed Cu-TiO2. The electrical resistivity of Cu in this study was $1.75 \times 10^{-8} \Omega m$ and that of FSPed Cu was $1.76 \times 10^{-8} \Omega m$; the FSPed Cu–TiO₂ surface composites treated at different GWs also maintained good electrical resistivity qualities up to 1.77 × 10^{-8} , 1.78×10^{-8} , and $179 \times 10^{-8} \Omega m$, respectively, for GW of 0.5, 1, and 1.5. The electrical resistivity would be directly proportional to grain size [29]. Additionally, Figure 8 shows little difference in electrical resistivity between the FSPed samples and pure Cu. Grain refining significantly increases the Cu strength through accumulative roll bonding without affecting the electrical resistivity [1]. The mean accessible route of electrons and heat carriers was improved due to the smaller grain size and the slightest change in electrical resistivity even after the TiO2 particle was added to Cu through FSP [27]. Second, the interface between TiO2 and Cu served as an electron transmission center and a thermal insulation barrier for heat flow (30f). Third, improving the quality of TiO₂ increases its electrical and thermal resistance.

The observed trend in electrical resistivity is due to a decrease in GW, which causes a reduction in the grain size and a more uniform distribution of reinforcement, which improves the reinforcement/matrix interface area. Genuine examples of surface flaws that scatter the traveling electron are grain boundaries and interfaces. Electrical resistivity increased along with GW because of the combined action. Finally, the variables increase the electrical resistivity of FSP composites with higher GW and vol% by 2.3% Ω m compared to pure Cu. No porosity is present within composites, the evenly dispersed TiO₂ forms a web of connected heat and

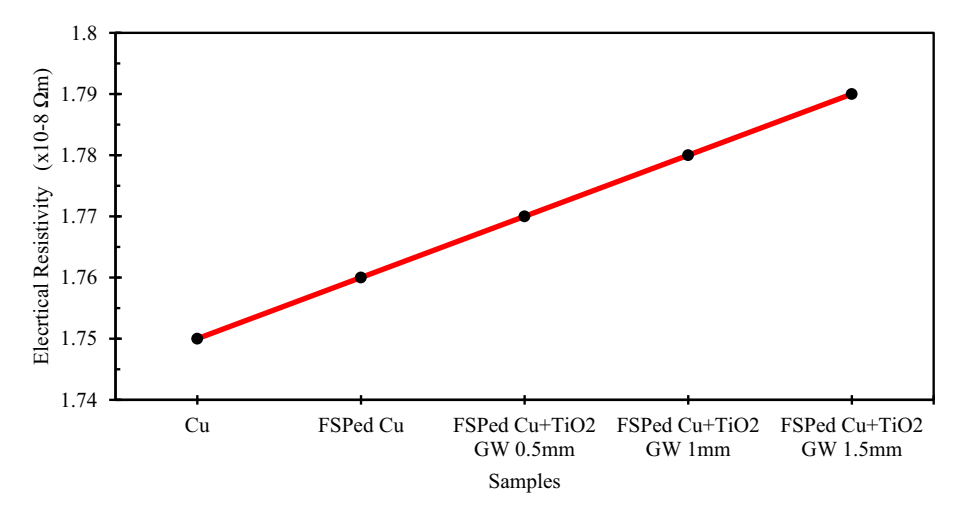


Figure 8: Variation of electrical resistivity against different samples.

electron carriers, and TiO₂ and the Cu matrix had better interfacial bonding.

4 Conclusions

Using FSP technology, pure Cu butt welds and a Cu-TiO₂ surface nanocomposite have been produced effectively with various reinforcement volume percentages and GWs. How FSP impacted the hardness, microstructure, wear, and electrical resistivity has been evaluated. The findings indicate the following: Surface composites with a flawless Cu-TiO₂ composition were created within the chosen parameter range. A Cu-TiO₂ surface compound with a volume percentage of 24% TiO₂ is 65% harder than the underlying material, with a microhardness of 121 HV. TiO₂ nanoparticles were uniformly distributed throughout the Cu matrix without forming agglomerates, with the stirred zone having significantly superior microhardness. The grain sizes of Cu reinforced with TiO2 are smaller than those of unreinforced welds. The study demonstrates that the use of FSP to distribute TiO₂ nanoparticles evenly throughout a copper matrix can significantly increase the wear resistance. The Cu–TiO₂ composite showed wear rates of 316 \times 10⁻⁵ and 175.31 \times 10⁻⁵ mm³·m⁻¹, respectively. The surface of FS-processed copper showed more plastic deformation with material removal, while the surface reinforced with TiO2 particles showed less deformation with shallow plowing. The composite material FSPed Cu-24% TiO2 is enhanced using FSP at a GW of 1.5 mm to increase its hardness, electrical conductivity, and wear resistance. The wear surface shows more plastic deformation, and the electrical resistivity increases with Cu–TiO₂ at maximum GW. This material is suitable for marine applications due to its high electrical resistivity.

The current study's path revealed a few areas that require more research: the effect of multi-pass, higher temperature, tool pin profile, reinforcements, and electrical resistivity on mechanical, tribological, and corrosion behavior. Studies of wear behavior are conducted by varying the applied loads, SDs, and speeds.

Acknowledgments: The authors extend their appreciation to the Deputyship for Research and Innovation, Ministry of Education in Saudi Arabia, for funding this research work through project no. IFKSUOR3-323-2.

Funding information: The authors extend their appreciation to the Deputyship for Research and Innovation, Ministry of Education in Saudi Arabia, for funding this research work through project no. IFKSUOR3-323-2.

Author contribution: All authors have accepted responsibility for the entire content of this manuscript and approved its submission.

Conflict of interest: The authors state no conflict of interest.

Data availability statement: The data analyzed in this manuscript are the part of our research work and is available for public use.

References

- [1] Naik, R. B., K. V. Reddy, G. M. Reddy, and R. Arockia Kumar. Development of high strength and high electrical conductive Cu and Cu–W composite by friction stir processing: Effect of traverse speed. *Proceedings of the Institution of Mechanical Engineers, Part C: Journal of Mechanical Engineering Science*, 2022, pp. 1–11.
- [2] Wąsik, M. and J. Karwan-Baczewska. Copper metal matrix composites reinforced by titanium nitride particles. *Key Engineering Materials*, Vol. 682, 2016, pp. 270–275.
- [3] Qi, W. X., J. P. Tu, F. Liu, Y. Z. Yang, N. Y. Wang, H. M. Lu, et al. Microstructure and tribological behavior of a peak aged Cu–Cr–Zr alloy. *Materials Science and Engineering: A*, Vol. 343, No. 1–2, 2003, pp. 89–96.
- [4] Hernández-Pérez, A., M. Eddahbi, M. A. Monge, A. Muñoz, and B. Savoini. Microstructure and mechanical properties of an ITER-grade Cu–Cr–Zr alloy processed by equal channel angular pressing. Fusion Engineering and Design, Vol. 98–99, 2015, pp. 1978–1981.
- [5] Purcek, G., H. Yanar, M. Demirtas, Y. Alemdag, D. V. Shangina, and S. V. Dobatkin. Optimization of strength, ductility and electrical conductivity of Cu–Cr–Zr alloy by combining multi-route ECAP and aging. *Materials Science and Engineering: A*, Vol. 649, 2016, pp. 114–122.
- [6] Wei, K. X., W. Wei, F. Wang, Q. B. Du, I. V. Alexandrov, and J. Hu. Microstructure, mechanical properties and electrical conductivity of industrial Cu–0.5%Cr alloy processed by severe plastic deformation. *Materials Science and Engineering: A*, Vol. 528, No. 3, 2011, pp. 1478–1484.
- [7] Li, J., J. Wongsa-Ngam, J. Xu, D. Shan, B. Guo, and T. G. Langdon. Wear resistance of an ultrafine-grained Cu-Zr alloy processed by equal-channel angular pressing. *Wear*, Vol. 326–327, 2015, pp. 10–19.
- [8] Surekha, K. and A. Els-Botes. Development of high strength, high conductivity copper by friction stir processing. *Materials & Design*, Vol. 32, No. 2, 2011, pp. 911–916.
- [9] Barmouz, M. and M. K. Givi. Fabrication of in situ Cu/SiC composites using multi-pass friction stir processing: Evaluation of microstructural, porosity, mechanical and electrical behavior. Composites Part A: Applied Science and Manufacturing, Vol. 42, No. 10, 2011, pp. 1445–1453.
- [10] Sathiskumar, R., I. Dinaharan, N. Murugan, and S. J. Vijay. Influence of tool rotational speed on microstructure and sliding wear behavior of Cu/B4C surface composite synthesized by friction stir processing. *Transactions of Nonferrous Metals Society of China*, Vol. 25, No. 1, 2015, pp. 95–102.

- [11] Avettand-Fènoël, M.-N., A. Simar, R. Shabadi, R. Taillard, and B. de Meester. Characterization of oxide dispersion strengthened copper based materials developed by friction stir processing. *Materials & Design*, Vol. 60, 2014, pp. 343–357.
- [12] Yaghoubi, M. A., N. Anjabin, and H. S. Kim. Effect of Y2O3 nanoparticles on the evolution of the microstructure and mechanical properties of severely plastic deformed Cu sheets during friction stir processing. *Metals and Materials International*, Vol. 29, 2023, pp. 2710–2725.
- [13] Khosravi, J., M. K.B. Givi, M. Barmouz, and A. Rahi. Microstructural, mechanical, and thermophysical characterization of Cu/WC composite layers fabricated via friction stir processing. *International Journal of Advanced Manufacturing Technology*, Vol. 74, 2014, pp. 1087–1096.
- [14] Sabbaghian, M., M. Shamanian, H. R. Akramifard, and M. Esmailzadeh. Effect of friction stir processing on the microstructure and mechanical properties of Cu–TiC composite. *Ceramics International*, Vol. 40, No. 8, Part B, September 2014, pp. 12969–12976.
- [15] Suvarna Raju, L. and A. Kumar. A novel approach for fabrication of Cu-Al2O3 surface composites by friction stir processing. *Procedia Materials Science*, Vol. 5, 2014, pp. 434–443.
- [16] Jafari, J., M. K.B. Givi, and M. Barmouz. Mechanical and microstructural characterization of Cu/CNT nanocomposite layers fabricated via friction stir processing. *International Journal of Advanced Manufacturing Technology*, Vol. 78, 2015, pp. 199–209.
- [17] Lakshminarayanan, A. K. and V. Balasubramanian. Process parameters optimisation for friction stir welding of AISI 409M grade ferritic stainless steel. *Experimental Techniques*, Vol. 37, 2013, pp. 59–73.
- [18] Salehi, M., M. Saadatmand, and J. A. Mohandesi. Optimization of process parameters for producing AA 6061/SiC nanocomposites by friction stir processing. *Transactions of Nonferrous Metals Society of China*, Vol. 22, No. 5, 2012, pp. 1055–1063.
- [19] Devaraju, A., A. Kumar, and B. Kotiveerachari. Influence of addition of Grp/Al2O3p with SiCp on wear properties of aluminum alloy 6061-T6 hybrid composites via friction stir processing. *Transactions* of Nonferrous Metals Society of China, Vol. 23, No. 5, 2013, pp. 1275–1280.
- [20] Samal, P., H. Tarai, A. Meher, B. Surekha, and P. R. Vundavilli. Effect of SiC and WC reinforcements on microstructural and mechanical characteristics of copper alloy-based metal matrix composites using stir casting route. *Applied Sciences*, Vol. 13, 2023, id. 1754.

- [21] Shahedi, B., M. Damircheli, and A. Shirazi. Experimental investigation of the effects of welding parameters and TiO2 nanoparticles addition on FSWed copper sheets. *Materials Research Express*, Vol. 6, No. 2, 2019, pp. 1–24.
- [22] Suvarna Raju, L. and A. Kumar. Influence of Al2O3 particles on the microstructure and mechanical properties of copper surface composites fabricated by friction stir processing. *Defence Technology*, Vol. 10, No. 4, 2014, pp. 375–383.
- [23] Kumar, S., N. Malik, P. Cinelli, and V. Sharma. High strain rate behavior of stir cast hybrid Al-Si matrix composites using split hopkinson pressure bar. *Silicon*, Vol. 16, 2024, pp. 231–240.
- [24] Kumar, H., R. Prasad, P. Kumar, and S. A. Hailu. Friction and wear response of friction stir processed Cu/ZrO₂ surface nanocomposite. *Journal of Nanomaterials*, Vol. 2022, 2022, id. 6767941, 12 pages.
- [25] Dadkhah, M., M. H. Mosallanejad, L. Iuliano, and A. Saboori. A comprehensive overview on the latest progress in the additive manufacturing of metal matrix composites: potential, challenges, and feasible solutions. *Acta Metall Sin (Engl Lett)*, Vol. 34, 2021, pp. 1173–1200
- [26] Sakthivel, T. and J. Mukhopadhyay. Microstructure and mechanical properties of friction stir welded copper. *Journal of Materials Science*, Vol. 42, No. 19, 2007, pp. 8126–8129.
- [27] Velmurugan, T., R. Subramanian, G. Suganya Priyadarshini, and R. Raghu. Experimental investigation of microstructure, mechanical and wear characteristics of Cu-Ni/Zrc composites synthesized through friction stir processing. *Arch Metall Mater*, Vol. 65, 2020, pp. 565–574.
- [28] Akinlabi, E. T., D. M. Madyira, and S. A. Akinlabi. Effect of heat input on the electrical resistivity of dissimilar friction stir welded joints of aluminium and copper. *IEEE Africon'11*, Victoria Falls, Zambia, 2011, pp. 1–4.
- [29] Mirjavadi, S. S., M. Alipour, S. Emamian, S. Kord, A. M. Hamouda, P. G. Koppad, et al. Influence of TiO2 nanoparticles incorporation to friction stir welded 5083 aluminum alloy on the microstructure, mechanical properties and wear resistance. *Journal of Alloys and Compounds*, Vol. 712, 2017, pp. 795–803.
- [30] Heidarpour, A., Y. Mazaheri, M. Roknian, and S. Ghasemi. Development of Cu–TiO₂ surface nanocomposite by friction stir processing: Effect of pass number on microstructure, mechanical properties, tribological and corrosion behavior. *Journal of Alloys and Compounds*, Vol. 783, 2019, pp. 886–897.
- [31] Sudhagar, S. and P. M. Gopal. Investigation on mechanical and tribological characteristics Cu/Si3N4 surface composite developed through friction stir processing. *Silicon*, Vol. 14, 2022, pp. 4207–4216.